HYDROLOGIC AND GEOLOGIC FACTORS AFFECTING LAND SUBSIDENCE NEAR ELOY, ARIZONA

Victoria J. Epstein

U.S. GEOLOGICAL SURVEY

Water-Resources Investigations Report 87-4143

Tucson, Arizona
September 1987

HYDROLOGIC AND GEOLOGIC FACTORS AFFECTING LAND SUBSIDENCE NEAR ELOY, ARIZONA

By

Victoria J. Epstein

ABSTRACT

At an extensometer site near Eloy, Arizona, 1.09 meters of land subsidence caused by ground-water withdrawal were measured by leveling in 1965-83. The extensometer, which partially penetrates the compressible sediments, recorded 0.82 meter of compaction during the same period. By use of a one-dimensional model, cumulative daily compaction values were simulated to within an average of 0.0038 meter of the actual values. Land subsidence was simulated to within an average of 0.011 meter using the same model in conjunction with geohydrologic data of the sediments below the extensometer. A highly compressible clay layer that is 24.38 meters thick was partially penetrated by the extensometer. The simulation indicated that the layer was driving compaction and land subsidence linearly with respect to time, despite the presence of other compacting layers. Because of its thickness and compressibility, this layer can be expected to continue to compact after applied vertical stresses have stopped increasing and other layers have stopped compacting. The sensitivity analysis indicated that the compressibility of fine-grained sediments (expressed as specific storage) is one of the factors to which compaction is most sensitive. The preconsolidation stress and hydraulic conductivity also affect land subsidence near Eloy, Arizona.

INTRODUCTION

Land subsidence caused by ground-water withdrawal may affect many alluvial basins in the Southwest. Near Eloy, Arizona, in the central part of Picacho basin, substantial land subsidence has occurred (fig. 1). Alluvial basins where land subsidence is occurring are characterized by highly compressible silt and clay deposits and large water-level declines caused by ground-water pumping that greatly exceeds natural recharge. Water-level declines create a vertical compressive stress that causes compaction of the fine-grained sediments. The compaction of subsurface deposits results in the lowering of the land surface, which is referred to as land subsidence.

Land subsidence and associated deformation of sediments in the alluvial basins of the Southwest have damaged manmade structures such as roads, pipelines, and well casings. Land subsidence may be a consideration in future ground-water management in the arid Southwest. This study is part of the second Regional Aquifer-System Analysis (RASA II) study designed by the U.S. Geological Survey to explore hydrologic problems, such as land subsidence, that were identified in an earlier RASA study of the Southwest alluvial basins of Arizona.

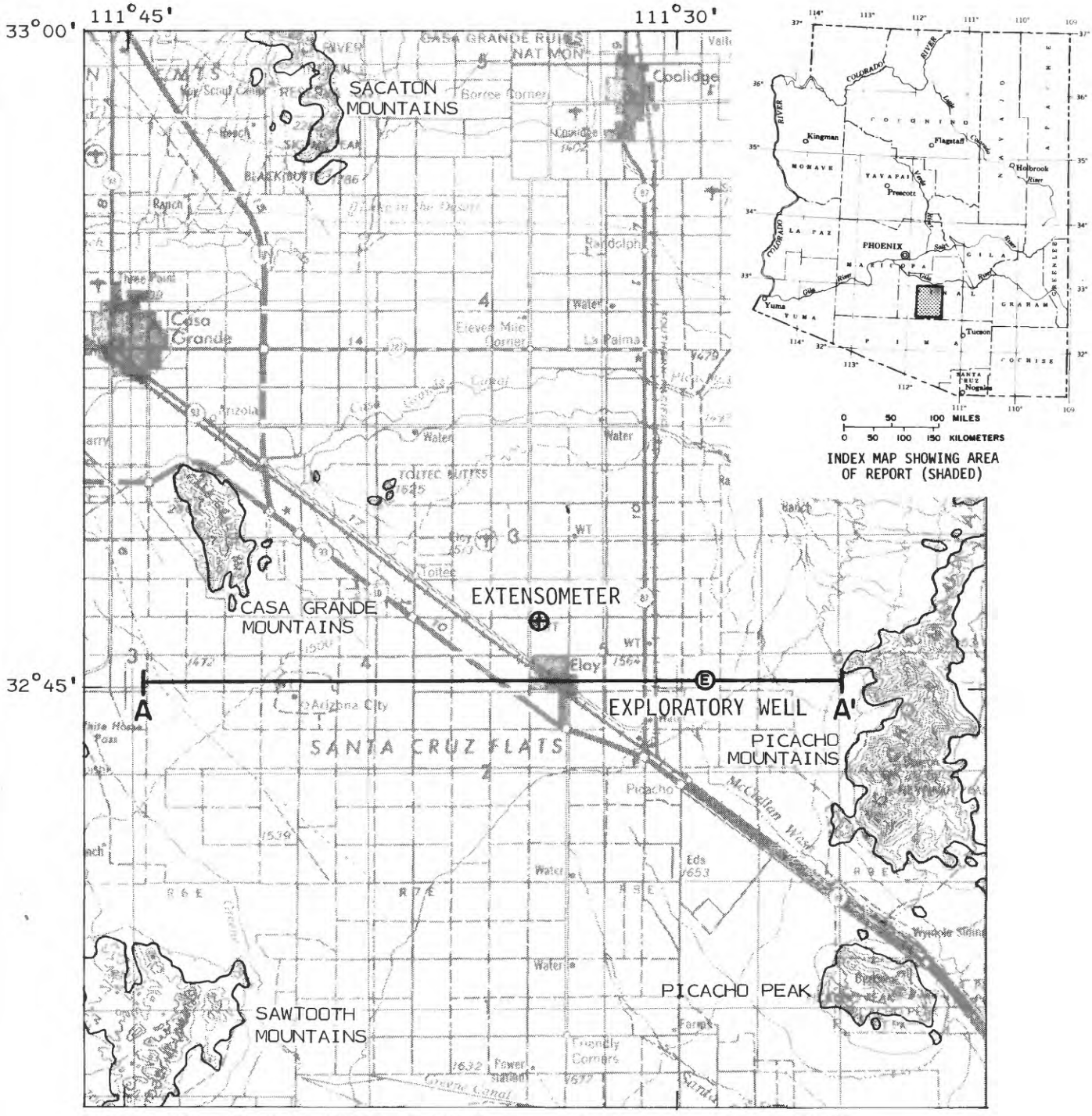

EXPLANATION

BEDROCK CONTACT

LINE OF SECTION

A A'

Figure 1.--Area of report (shaded).

Purpose and Scope

This report describes the results of a study to analyze geologic and hydrologic factors affecting compaction of sediments near Eloy, Arizona (fig. 1). A vertical extensometer installation in northwest Eloy has recorded compaction and ground-water levels since 1965 (fig. 1). From 1965 to 1983, 0.82 m of compaction was measured in the upper 252 m of sediments. During the same period, 1.09 m of land subsidence at the extensometer was measured by leveling (Schumann, 1986). Land subsidence exceeds measured compaction as a result of deformation of predominantly fine-grained sediments below the bottom of the extensometer (Schumann and Poland, 1970).

Geologic interpretations were made on the basis of available lithologic data. The geologic interpretations and compaction record were assimilated with hydrologic data to construct a model of vertical compaction for the extensometer site near Eloy, Arizona.

Approach

Geophysical logs, drill cuttings, drillers' logs, and grain-size analyses were used to define the geology of Picacho basin. On the basis of this analysis, the type and extent of compacting sediments below the extensometer are defined. A one-dimensional numerical model developed by Helm (1972, 1975, and 1976) and a sensitivity analysis was used to quantitatively analyze compaction of sediments at the extensometer site near Eloy. Input for the model includes stress changes determined from water levels measured at the well and hydrologic and geologic properties. Hydraulic conductivity and porosity were estimated from laboratory analyses of sediments from the extensometer site. The model was calibrated by altering input parameters and comparing results with the historical compaction record. Model sensitivity was determined by comparison of the alteration of several geologic and hydrologic properties by given increments. The sensitivity analysis also established the effect of each property on the compaction process.

Terminology

Compaction, as used in this report, is a decrease in thickness of a layer in response to an increase in vertical compressive stress (Poland and others, 1972). Compaction includes both instantaneous and time-dependent deformation. Compaction that is time dependent, is synonymous with the term consolidation as used by soil engineers. Consolidation is used only when referencing a consolidation test. Aquitard refers to "a saturated but poorly permeable bed that impedes ground-water movement and does not yield water freely to wells, but which may transmit appreciable water to and from adjacent aquifers and, where sufficiently thick, may constitute an important storage unit" (Poland and others, 1972). Aquifer system includes aquitards and aquifers. The terms, virgin specific storage and elastic specific storage are unrecoverable and recoverable specific storage, respectively, as used by Helm (1975).

Data-Collection Site

The extensometer site near Eloy consists of a pipe and weighted cantilever. The pipe rests on a steel weight at the bottom of the well, which is 252 m below land surface, and is counter weighted by a fulcrum and lever at the top of the well. As the sediments compact, the pipe appears to move up relative to the well casing. The movement is measured on a recorder at a 10:1 scale. From 1965 to 1979, the extensometer consisted of a taut cable anchored to the steel weight. The change from cable to pipe was made to improve the compaction record; less friction occurs between the pipe and the well as a result of the stiffness of the pipe. The lever and counterweight system help prevent the pipe from bending under its own weight, which would cause more points of contact. Friction in an extensometer is indicated by a stairstep pattern in the compaction record. With the conversion from cable to pipe, much of the friction was eliminated. In a deep well, such as at the extensometer site, a totally friction-free installation probably is not attainable.

HYDROLOGY

Water-level measurements from wells near the extensometer site extend back to 1923 when water levels began to decline because of ground-water pumping (Hardt and Cattany, 1965). From spring 1923 to spring 1942, water levels declined about 9 m in Eloy. From 1940 to 1963, water-level decline accelerated to 1.8 m/yr and the overall decline was 44 m (Hardt and others, 1964; Hardt and Cattany, 1965). From 1965 to 1983, water levels at the extensometer site declined 15.2 m at an average rate of 0.79 m/yr.

Hardt and Cattany (1965) reported water-level fluctuations of 6 to 15 m/yr in the Picacho basin. Most water levels are obtained from wells that are shallow in relation to the well at the extensometer site. These wells extend to a depth of 183 m and have more extensive perforated intervals than the well at the extensometer site. The extensometer well is perforated from 171 to 177 m below the land surface, and the water-level fluctuations range from 15 to 30.5 m/yr. The difference between the extensometer water-level fluctuations and water-level fluctuations reported by Hardt and Cattany (1965) may indicate that water-level fluctuations near Eloy are predominantly artesian-pressure fluctuations.

Water-level distribution with depth is not known; therefore, the aquifer system at the extensometer site is assumed to be unconfined for the compaction simulation. The fine-grained layers above the bottom of the extensometer are assumed to be aquitards that are not horizontally extensive enough to impede ground-water flow. The effect of this assumption is discussed in the section entitled "Results."

GEOLOGY

Picacho basin is bounded by the Sawtooth Mountains to the southwest, the Picacho Mountains to the east, the Casa Grande Mountains to the west, and the Sacaton Mountains and the town of Coolidge to the north (fig. 1). The geology of Picacho basin was defined by analysis of

drillers' logs, well cuttings, geophysical data, and grain-size distributions. A study of the generalized regional geology defined the depth of compacting sediments, which, in turn, were studied in detail. In the Eloy area, the basin probably is more than 3,000 m deep on the basis of an exploratory well east of Eloy (fig. 1). Bedrock composed of Precambrian quartz-diorite gneiss was encountered at a depth of 3,001 m (Eberly and Stanley, 1978). Picacho basin is filled with sediments deposited before and after the Basin and Range disturbance (fig. 2), which was a period of block faulting in late Miocene time (Scarborough and Peirce, 1978). The disturbance created a horst-and-graben topography. Sediments accumulated in the basins during the Cenozoic Era (Eberly and Stanley, 1978).

Mountains surrounding Picacho basin are composed of gneissic, granitic, and volcanic rocks. Lithologic information from an exploratory well north of the extensometer site indicates that a reddish-brown conglomerate containing fragments of a quartz-diorite gneiss overlies the bedrock in the center of the basin. The conglomerate is at a depth of 2,946-3,001 m. Volcanic rocks that overlie the conglomerate at 2,765-2,946 m consist of a purplish basalt and an ultrapotassic trachyte dated at 15 and 17 million years (m.y.) ago, respectively (Eberly and Stanley, 1978). Another layer of reddish-brown conglomerate containing fragments of volcanic rocks is at a depth of 2,522-2,743 m. This conglomerate is unlike the lower conglomerate in that it contains volcanic fragments that may be associated with the Basin and Range disturbance. Thick evaporite deposits of anhydrite are at a depth of 707-2,522 m, and a reddish-brown clay deposit is at 198-707 m. The clay and anhydrite deposits may have formed in a closed-drainage basin and in a shallow lake environment. Through-flowing streams such as the Santa Cruz River subsequently deposited alluvial sediments in the basin (Scarborough and Peirce, 1978). These sediments are composed of gravel, sand, and silt and extend 213 m below the land surface.

Although the bedrock is 3,001 m below the land surface in the deepest part of the basin, analyses of drill cuttings indicate that sediments deeper than 305 m are incompressible. At about this depth, well cuttings changed from unconsolidated silt and clay to mudstone. Many drillers' logs referred to this sediment as shale or hardrock. For the purpose of this study, the deposits in the upper 305 m of sediments can be divided into three units (fig. 2). Unit I, the upper unit, is 0-107 m thick and consists of coarse sand and gravel. Unit II is 30-122 m thick and consists of fine- to coarse-grained sand, silty lenses, and some gravel. Unit III is clayey silt to silty clay, 0-488 m thick, and may extend below 305 m in the center of the basin.

The depth and areal distribution of Units I and II are almost constant throughout the basin in relation to Unit III. Although Unit III is not present at the edges of the basin, it is the thickest unit in the center of the basin. The conglomerate that contains volcanic fragments lies at shallow depths on the edges of the basin; however information on composition, thickness, and permeability of the conglomerate is limited.

Unit I is mainly coarse sand and gravel composed of rounded to subrounded grains of granite, basalt, quartz and quartzite. The granite fragments contain orthoclase feldspar that gives the sediment a pink hue. Weathering of some iron-rich minerals stains the grains of quartz an orange color. In general, the unit is pinkish white to pinkish gray.

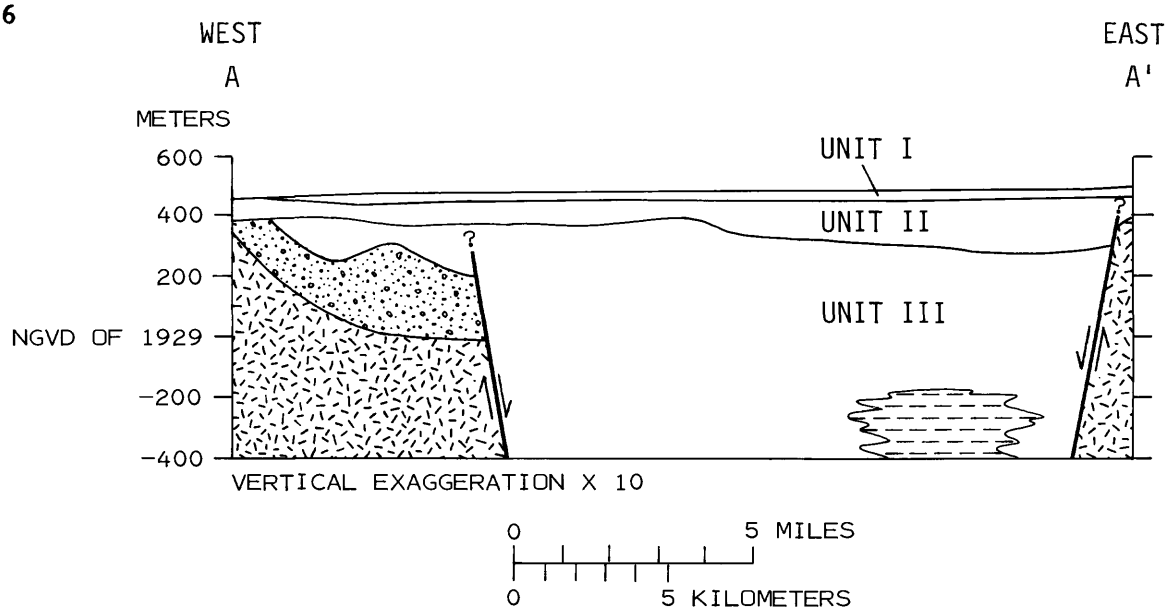

E X P L A N A T I O N

UNIT I	SAND AND GRAVEL
UNIT II	SILTY SAND AND GRAVEL
UNIT III	SILTY CLAY AND MUDSTONE
	CONGLOMERATE
	ANHYDRITE
	BEDROCK
?	FAULT—Arrow indicates movement at fault block. Queried where uncertain

Figure 2.--Generalized geologic section A-A' of Picacho basin. Location of section A-A' is shown in figure 1.

Unit II contains fine to medium sand, traces of gravel, and silt lenses. Feldspar, quartz, and muscovite are common minerals. Fewer igneous clasts are present relative to Unit I, and grains are more angular. Unit II generally is pink to light reddish brown. The silt lenses are rich in muscovite or sometimes biotite and are 1-6 m in thickness.

Unit III consists of lacustrine silts, clays, evaporites, and gravel stringers. Silty lenses increase in thickness and become increasingly rich in clay at depth. The sediments change with depth from light reddish brown brown to reddish brown and eventually become red brown. Gypsum, which is present initially as white opaque flakes, increases in concentration with depth. Lower parts of Unit III contain 10 to 90 percent clear euhedral gypsum. The clay mineral fraction is predominantly montmorillonite. Silt-sized material is quartz, gypsum, muscovite, and lesser biotite. In the center of the basin, where it extends below a depth of 305 m, Unit III is a lithified siltstone and claystone unit.

THEORY OF STRESS AND COMPACTION

Effective Stress

Declines in ground-water levels caused by pumping can increase effective stresses that cause aquitards to compact. An unconfined aquifer system is at equilibrium when fine-grained layers are not compacting despite the presence of downward effective stresses. The system at equilibrium has a net downward stress equal to the weight of the sediments above the water table and the bouyant weight of the sediments below the water table. Bouyant weight is the weight of the sediments minus the weight of the displaced water. When the water table is lowered, the weight of the dewatered zone changes from a bouyant weight to an unsaturated weight. Because the unsaturated weight is larger than the bouyant weight, the stress on the sediments below the dewatered zone is increased. In a confined system, effective stresses are increased by a decrease in pore-water pressure, and total applied stresses remain constant.

Terzaghi (1943) developed equations to describe the stresses in a system at equilibrium:

$$P_a = U + P', \tag{1}$$

where

P_a = applied stress,
U = pore-water pressure, and
P' = effective stress.

Stress changes in an unconfined system are:

$$\Delta P_a = \Delta U + \Delta P'. \tag{2}$$

Stress changes in a confined system are:

$$\Delta P_a = 0 \tag{3}$$

$$\Delta U = -\Delta P'. \tag{4}$$

Seepage stress, which is produced by the presence of hydraulic gradients across slow-draining layers, also contributes to effective stress in a confined system (Poland and others, 1972).

Effective stress changes in aquitards in an unconfined system are not instantaneous. The initial increase in applied stress is transferred to the pore water. As water flows out of the layer, the pore-water pressure is decreased and the load is transferred to the sediment skeleton as effective stress. The particles rearrange to form a more dense packing in order to reestablish equilibrium. A decrease in porosity accompanies the rearrangement causing compaction and expulsion of water.

In an unconfined system, a change in the water table ultimately produces a change in effective stress at depth z, which is below the lowest elevation of the water table, equal to the change in weight of the dewatered zone. The effective-stress change can be calculated as the change in weight per unit area:

$$\Delta w = -\Delta h(\gamma_m - \gamma_b), \tag{5}$$

where

Δw = the change in weight of the column,
Δh = the change in height of the water table,
γ_m = the unsaturated unit weight of sediments, above depth, z, and
γ_b = bouyant unit weight of sediments.

In a confined system, a change in water level produces a change in effective stress equal to the unit weight of water multiplied by the height of water-level change. In both systems, the water-level record can be used to calculate ultimate changes in effective stress.

Stress-Compaction Relations

The type of compaction occurring at any given time is a function of the effective stress. All deposits have a preconsolidation stress, which is the past maximum effective stress. Compaction in response to an increase in applied stress is elastic if the applied stress increase is less than the preconsolidation stress. Compaction is termed virgin if the applied stress is increased beyond the preconsolidation stress.

A normally consolidated sediment is one in which the preconsolidation stress is equal to the effective stress. Generally, compaction in normally consolidated sediments is elastic and small until the preconsolidation stress is reached. Compaction is larger and virgin after the preconsolidation stress is reached. Subsequent unloading produces small amounts of elastic expansion. Reloading produces elastic compaction until the past maximum effective stress is reached again.

Elastic compaction generally is recoverable and occurs instantaneously in highly permeable sediments, such as coarse-grained

sediments. Elastic compaction in fine-grained sediments is a slower process. Virgin compaction generally has a small component of elastic compaction and a larger component of nonrecoverable compaction. Virgin compaction in aquitards is approximately proportional to the logarithm of effective stress increase. Compaction in fine-grained sediments is time dependent and involves the slow expulsion of water and the corresponding increase in effective stress (Poland and others, 1972). In most cases, coarse-grained sediments, such as sand and gravel, that undergo virgin compaction have small inelastic components in relation to elastic components.

Effective stresses at a given depth within a sediment change in response to water-level fluctuations. A decrease in the water level increases the effective stress at a point below the initial level of the water table, and an increase in water level decreases the effective stress at such a point. Water levels typically fluctuate seasonally, and the processes of rebound and compaction may overlap. This stress-compaction relation, although complicated, can be quantified for an aquifer system by using a stress-compaction plot (Riley, 1969). The plot represents head changes in the aquifer system and compaction measured between the land surface and the bottom of the extensometer pipe.

For a cyclically fluctuating water-level system, stress, which is measured in meters of water, is plotted against compaction, which is measured in meters (fig. 3). Most plots consist of hysteresis loops that represent periods of elastic rebound or compaction caused by stress changes below the preconsolidation stress. Curves that connect the loops represent periods of virgin compaction, which occur when water levels fall and exceed the preconsolidation stress.

The stress-compaction diagram varies for each aquifer system; however, the diagram generally has a cyclic pattern. Systems with large disparities in layer thickness and properties may have unusual stress-compaction diagrams. For example, the stress-compaction diagram for the extensometer near Eloy (fig. 3) has open hysteresis loops. The open hysteresis loops probably are created when ongoing compaction in a thick layer, such as Unit III, overlaps with expansion in smaller layers, such as those in Unit II.

Stress-compaction relations can be quantified using the stress-compaction diagram. Because compaction is related to a change in volume of water, the stress-compaction slope can be related to the storage of an aquifer system (Riley, 1969). A specific-storage value can be calculated by dividing the inverse slope by the thickness of compacting layers (Riley, 1969). Elastic specific storage is the inverse slope of the hysteresis loops divided by the total initial thickness of the compacting sediments. The virgin specific storage is the inverse slope of the curve that connects loops divided by the total original thickness of compacting layers (fig. 3). The compressibility of the material is equal to the virgin specific storage divided by the unit weight of water.

Specific storage and compressibility values obtained from stress-compaction diagrams are useful in calculating system compaction in response to an increase in stress. Values derived from data that include compaction of more than one bed are composite values. Actual values for each bed probably are different.

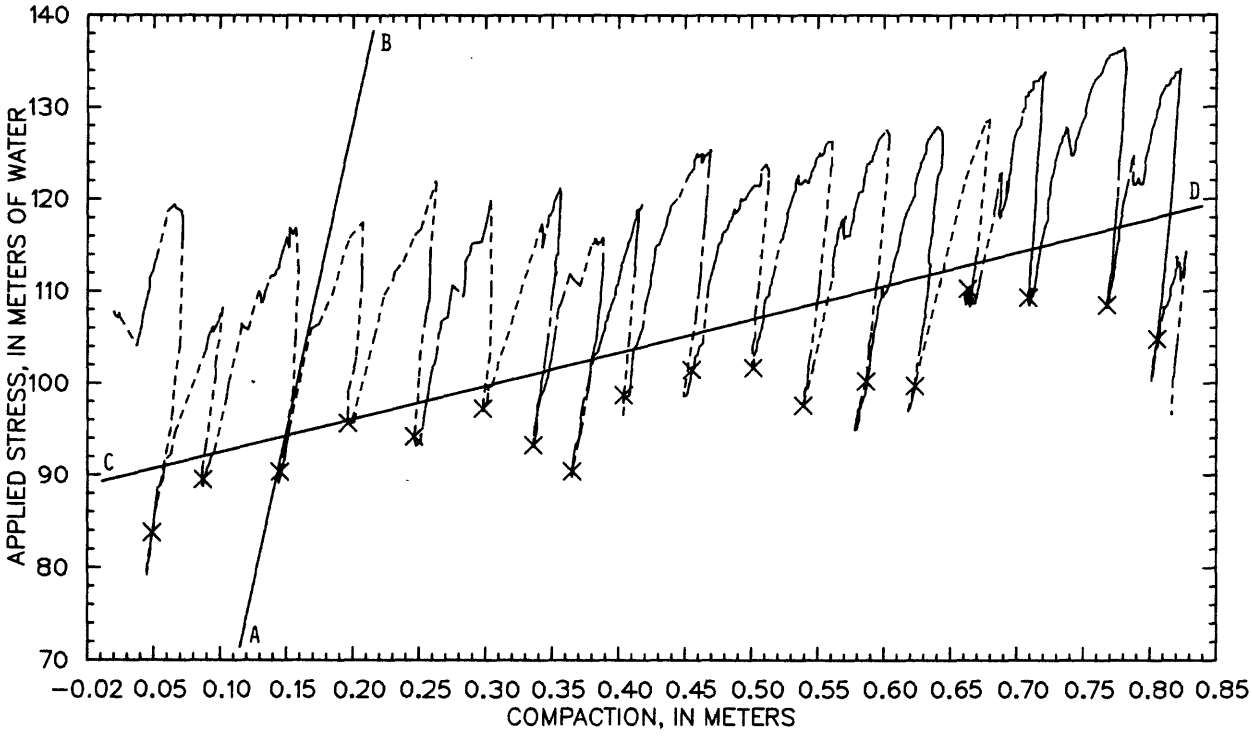

Figure 3.--Stress-compaction relation near Eloy, Arizona. The inverse slope of line A-B is elastic storage and the inverse slope of line C-D is virgin storage. X's mark the beginning of a calendar year.

The stress-compaction relation, quantified by the specific storage, is used in the calculation of compaction. A change in effective stress and a subsequent change in storage are related to a change in thickness that occurs when water is expelled from the sediment. Helm (1972) presents the following equation for calculating aquifer compaction:

$$b_c = \int_0^t \int_0^b (S_s) \frac{\partial(\Delta P')}{\partial t} \, dz \, dt, \qquad (6)$$

where

b_c = compaction,

t = time,

b = original thickness of layer,

S_s = specific storage, and

z = depth from top of layer.

Specific storage, S_s, is elastic specific storage or virgin specific storage depending on the value of the effective stress in relation to the preconsolidation stress. When the effective stress exceeds the preconsolidation stress, a virgin specific-storage value is used. When the

effective stress is less than the preconsolidation stress, the elastic specific-storage value is used.

Certain assumptions are made in the calculation of compaction. Because the compressibility of the soil skeleton is much larger than the compressibility of the grains and water, the grains and water are assumed to be incompressible. Compaction, therefore, is equal to the change in volume of the voids due to water being expelled. The assumption was made that compaction is vertical and has no horizontal components. Land subsidence is assumed to be the sum of the compaction of each layer of the subsurface column.

Compaction of fine-grained sediments in response to a change in effective stress generally is time dependent. The time required for a given amount of compaction to occur is a function of the hydraulic conductivity, storage, and thickness of the aquitard. A unique time constant may be defined from the physical and hydraulic properties of an aquitard (Riley, 1969):

$$\tau = \frac{S_s(H_{dr})^2}{K}, \qquad (7)$$

where

τ = time constant,

H_{dr} = length of the drainage path, and

K = hydraulic conductivity.

The time constant is the time required to dissipate 93 percent of the excess pore pressure in the aquitard after an instantaneous increase in applied stress. At any point in time after an increase in applied stress, the percentage of the total compaction that has occurred is equal to the elapsed time divided by the time constant. Compaction can be calculated at each point in time by multiplying the degree of compaction by the total compaction that will ultimately occur due to a given stress change.

The time constant is partly a function of the hydraulic conductivity. The rate of compaction, therefore, is controlled by the rate at which water can be expelled from a layer. Low-permeability deposits compact at a slower rate than high-permeability deposits. Compaction in fine-grained sediments typically is time dependent, and compaction in coarse-grained sediments is nearly instantaneous.

HYDROLOGIC AND GEOLOGIC FACTORS

Several hydrologic and geologic factors have important effects on compaction in an aquifer system. Hydrologic factors include hydraulic conductivity and elastic and virgin specific storage. Geologic factors include grain-size distribution and aquitard thickness.

The hydraulic conductivity of a deposit controls the compaction rate. An increase in hydraulic conductivity increases the compaction rate. Specific storage affects the ultimate amount of compaction that can occur. An increase in specific storage will increase the total compaction that will ultimately occur in response to an increase in stress.

Several combinations of hydraulic conductivity and specific storage are possible in compacting sediments. Each combination is a function of the grain-size distribution of a sediment. For example, sediments rich in clay-size particles tend to have low hydraulic-conductivity values but high specific-storage values. Compaction in clay-rich deposits occurs in fairly large amounts that are spread out through time. These layers may continue to compact long after applied stresses have stopped increasing. Coarse-grained sediments that are composed mainly of sand and gravel have higher hydraulic-conductivity and lower specific-storage values than do clay sediments. Sand and gravel sediments can compact almost instantaneously; however, the compaction generally is small.

The thickness of a compressible layer affects the amount of time required for compaction to occur. As thickness increases, the length of the drainage path (H_{dr}) over which a given amount of water must travel in order to be expelled from a layer increases. Several small clay layers will dissipate all excess pore pressures and stop compacting before a single large clay layer with similar properties.

The boundaries of a deposit also affect compaction. A layer bounded above and below by aquifer material has symmetrical drainage around a no-flow midplane. A layer with an impermeable boundary can drain only in one direction. For example, in Picacho basin where bedrock is deep, the lower boundary of thick highly compressible deposits is the depth at which they are too lithified to compact. Because the lower boundary of the layer is impermeable, water can drain only out of the top of the layer. The length of the drainage path (H_{dr}) is twice that of a doubly draining bed of equal thickness, and the time constant is increased according to the square of H_{dr}.

On the basis of the regional and local geology, the compaction of each unit in response to a stress can be estimated. Unit I, which is predominantly coarse-grained sand and gravel, can be expected to compact elastically. Lenses of fine sand and silt in Unit II have lower permeabilities and higher specific storage than the coarse-grained material. Unit II probably is more compressible than Unit I in the virgin-stress range but probably compacts at a slower rate. Unit III, which is massive and thick, has a high clay mineral content and is more compressible in the virgin-stress range than Units I and II. These factors indicate that Unit III probably will compact more than Units I and II and for longer periods of time.

SIMULATION OF AQUIFER-SYSTEM COMPACTION AND LAND SUBSIDENCE NEAR ELOY

The one-dimensional compaction model developed by Helm (1972) was selected for simulation of compaction at the extensometer site near Eloy. The model computes the time distribution of compaction in a layer using boundary-stress values, hydraulic conductivity, specific-storage (or compressibility) values, and layer thickness.

Changes in applied stress at the boundary of a compacting layer can be calculated from measured changes in ground-water levels (Lofgren, 1969). The vertical effective-stress distribution within a layer is determined from the applied stress by solving the linear partial-differential equation:

$$\frac{\partial u}{\partial t} - \frac{\partial Pa}{\partial t} = \left(\frac{K}{S_s}\right)\frac{\partial^2 u}{\partial z}. \qquad (8)$$

The term, $\partial Pa/\partial t$, drops out at time zero because the load at the boundary is assumed to be applied instantaneously and held constant. The equation simplifies to Terzaghi's formulation of the diffusion equation:

$$\frac{\partial u}{\partial t} = \left(\frac{K}{S_s}\right)\frac{\partial^2 u}{\partial z^2}. \qquad (9)$$

Equation 9, which represents the distribution of pore pressure within the compacting layer, can be written in terms of effective stress (within the layer $\partial u/\partial t = -\partial P'/\partial t$):

$$\frac{\partial P'}{\partial t} = \left(\frac{K}{S_s}\right)\frac{\partial^2 P'}{\partial z^2}, \qquad (10)$$

where

S_s = elastic specific storage when P' is less than the preconsolidation stress and virgin specific storage when P' exceeds the preconsolidation stress.

Helm (1972) uses a time-centered finite-difference approximation of equation (3) and the Thomas algorithm, a forward and backward substitution method (Remson and others, 1971), to solve the set of equations for the effective stress at each node. The program defines which value of S_s is used on the basis of the value of P' in relation to preconsolidation stress (*pmax*) (Helm, 1972, 1975, 1976).

The vertical profile at the extensometer site was divided into discrete elements with a thickness of Δz. Changes in effective stress and storage are computed at a node located at the center of the element. Storage of each element is then calculated from the change in effective stress at each node using the appropriate value of S_s. The total compaction is the sum of the element storage multiplied by the thickness of the element (Δz):

$$b_c = \Delta z[0.5S_{skv} \sum_{j=1}^{J} (\Delta P'^{n}_{vj}+\Delta P'^{n}_{vj+1}) - 0.5S_{ske} \sum_{j=1}^{J} (\Delta P'^{n}_{ej}+\Delta P'^{n}_{ej+1})], \quad (11)$$

where

j = the node number,

n = time,

S_{skv} = virgin specific storage,

S_{ske} = elastic specific storage,

$pmax$ = preconsolidation stress,

P' = effective stress,

$\Delta P'^{n}_{ej}$ = $pmax^{n}_{j}$ - P' (e=elastic), and

$\Delta P'^{n}_{vj}$ = $pmax^{n}_{j}$ - $pmax^{o}_{j}$ (v=virgin).

When P' = $pmax$, the second term in the brackets drops out; and when P'^{n}_{j} is less than $pmax^{n}_{j}$, $pmax^{n}_{j}$, is set equal to $pmax^{o}_{j}$, the first term drops out.

Model Input

Input for the one-dimensional model includes applied stress changes, which are computed from water-level changes at upper and lower boundaries. Aquitard properties are layer thickness, hydraulic conductivity, and elastic and virgin specific storage. Aquifer properties are thickness of coarse-grained material, specific storage, average bouyant-unit weight, and average unsaturated-unit weight. Initial stress conditions are input as initial water level, preconsolidation stress, and preconsolidation-stress distribution.

At the extensometer site, the water-level record has many gaps that were filled in with linearly interpolated data to provide a continuous daily record. Changes in stress values determined from the daily record generally occur over periods of more than 1 day. Time steps of 1 day improve the accuracy of the calculations because changes in stress values occur over slightly longer time periods. Computational errors caused by changing from one specific-storage value to another during a time step generally are smaller with smaller time steps. Initial stress conditions were set to the initial water level or depth to water.

Each compacting layer was simulated separately. Although the model allows for using a weighted thickness of sediments, the silty lenses are sufficiently different from the silty-clay sediment of Unit III to warrant separate treatment. Seven separate layers are defined. Layers 1-6 are in Unit II, and layer 7 is in Unit III (fig. 4). The sediments in Unit I are not compressible in relation to the silt and clay layers in

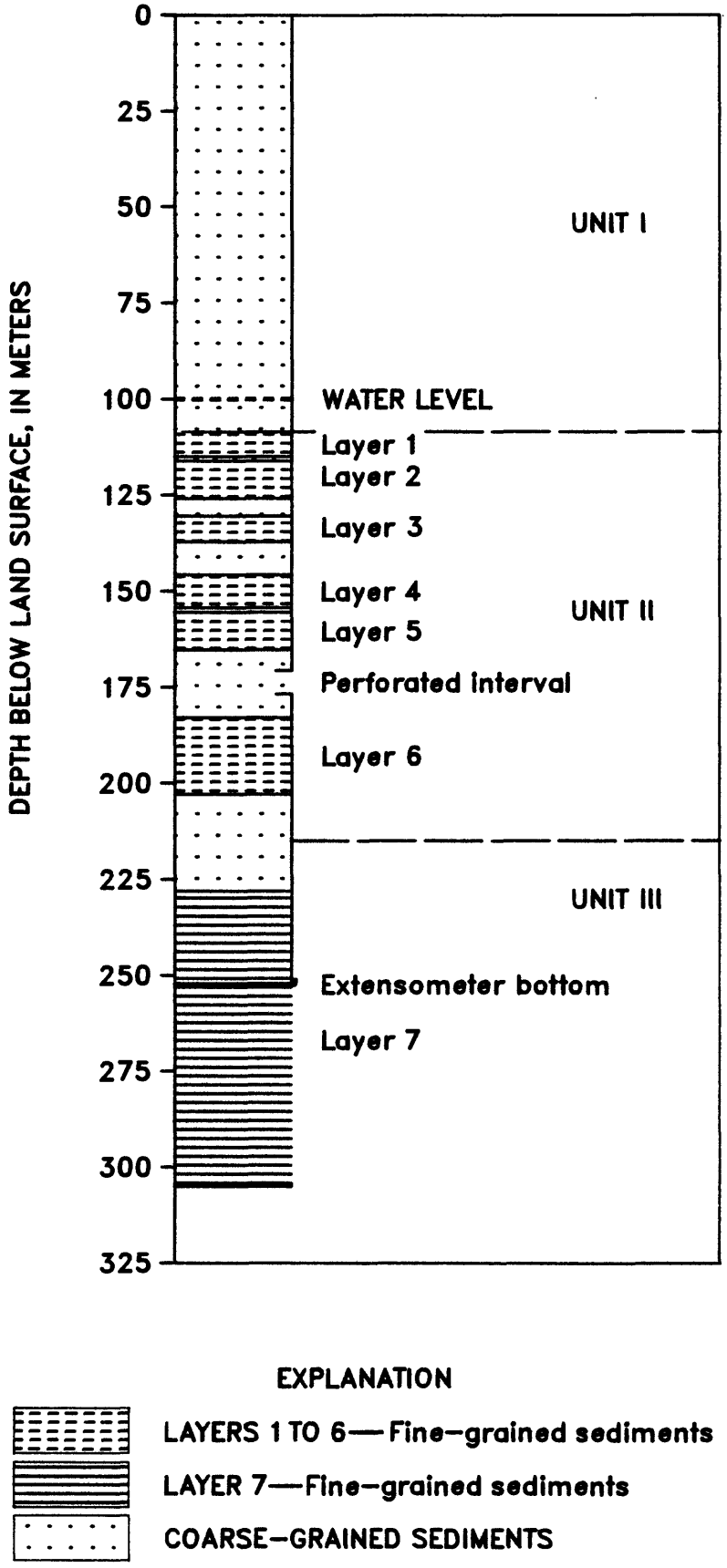

Figure 4.--Simulated compacting layers for the extensometer site near Eloy, Arizona.

Units II and III. The coarse sediments in Unit I, and the coarse sediments between the compressible layers in Units II and III are modeled as aquifer material. The thickness of these sediments is the sum of the thickness of material that is not in the aquitards. The aquifer material has low elastic and virgin specific-storage values and a high hydraulic conductivity in relation to the aquitard material. These sediments undergo little compaction, which is added to the aquitard compaction.

The thickness of each layer was determined from a detailed lithologic log of the well and an electric log. The silt lenses in Unit II are modeled as doubly draining layers of limited horizontal extent. Layer 7 is simulated as a singly draining layer with a no-flow lower boundary at 305 m below the land surface where sediments are estimated to be incompressible. To compare model output with the extensometer measurements, only the compaction occurring in the part of layer 7 penetrated by the well is added to the compaction computed in the other layers.

In order to simulate layer 7 as a singly draining layer, layer 7 is defined as a clay layer overlying an impermeable boundary. According to soil theory, a doubly draining layer has a symmetrical effective stress distribution around a no-flow boundary at the midplane. This convention can be used to simulate a singly draining layer by assuming that the layer is equivalent to the upper half of a doubly draining layer of twice the thickness. The no-flow boundary of the doubly draining layer is the lower impermeable boundary of the singly draining layer (fig. 5). Half the compaction of the imaginary doubly draining layer is equivalent to the compaction of the singly draining layer. The model was modified to calculate compaction in the upper 25 m of layer 7 as well as for the entire layer to a depth of 305 m.

The initial values for hydraulic conductivity were assigned on the basis of values determined in the U.S. Bureau of Reclamation laboratory. The storage coefficients are determined using the stress-compaction plot from the method described by Riley (1969). The coefficients estimated by Riley's method probably are average values of compacting beds with geologic and hydrologic properties of Units II and III. The layers in Unit II (1-5) were assumed to have a slightly lower-than-average specific storage, and the clay-rich layer (layer 7) was assumed to have a slightly higher value. Although layer 6 is in Unit II, it has properties that are between those of Units II and III. Layer 6 contains a slightly higher percentage of clay-size particles than layers 1-5. Layer 6 therefore is assigned a virgin specific-storage value slightly higher than that of layers 1-5, but lower than that of layer 7. Calibrated values of parameters used as input to the model are listed in table 1.

Preconsolidation stresses were estimated partly by the use of laboratory tests conducted in 1965 and by certain assumptions. The results of the laboratory tests indicate that the samples in 1965 were normally consolidated. This conclusion is verified by annual depth-to-water data for 1965 that indicated that water levels had declined 55 m and created large effective stresses. The tests, however, also indicated that the preconsolidation stress decreased significantly with depth in layer 7. Sediments within the same bed have a previous maximum stress

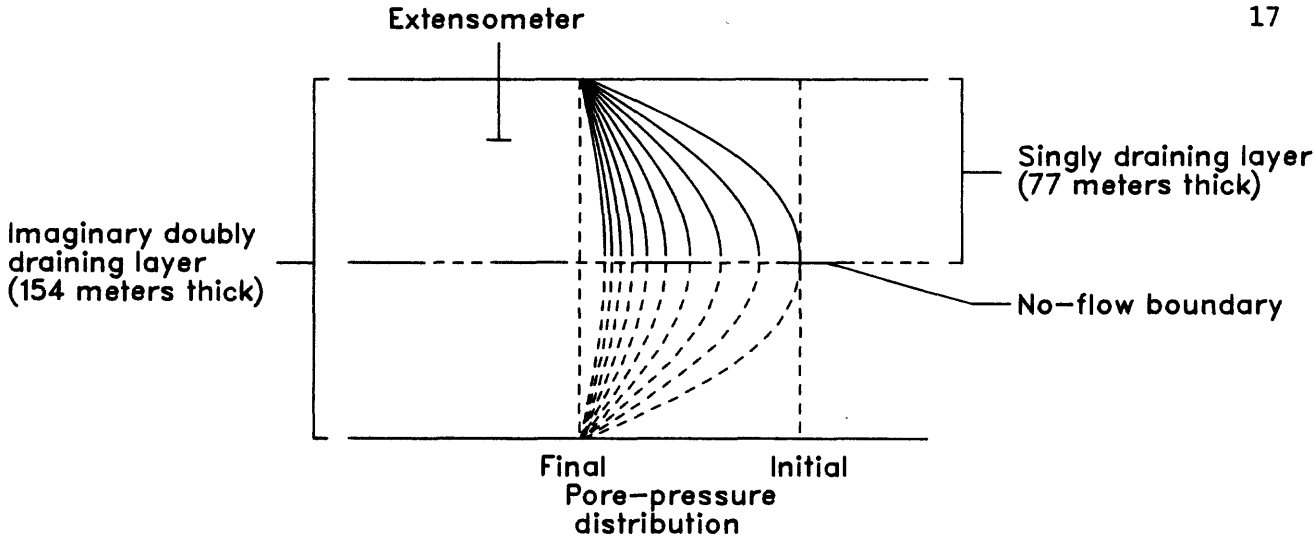

Figure 5.--Pore-pressure distribution in layer 7.

Table 1.--*Calibrated input values of specified parameters for the one-dimensional compaction model*

Layer number	Thickness, in meters	Specific storage, in meters^{-1}		Hydraulic conductivity, in meters per year	Preconsolidation stress, in meters[1]
		Elastic	Virgin		
1	5.49	1.0×10^{-5}	5.0×10^{-4}	2.0×10^{-2}	112.0
2	9.75	1.0×10^{-5}	5.0×10^{-4}	2.0×10^{-2}	112.0
3	6.71	1.0×10^{-5}	5.0×10^{-4}	2.0×10^{-2}	112.0
4	8.54	1.0×10^{-5}	5.0×10^{-4}	2.0×10^{-2}	112.0
5	9.75	1.0×10^{-5}	5.0×10^{-4}	2.0×10^{-2}	112.0
6	20.00	8.0×10^{-6}	6.0×10^{-4}	2.0×10^{-2}	113.5 104.7
7	24.38	1.0×10^{-5}	9.0×10^{-4}	1.5×10^{-2}	113.5 34.0

[1]Preconsolidation stress is for 1963, and is expressed as depth to water below land surface. More than one value indicates a range of values from the edge to the center of the layer.

(preconsolidation stress) distribution equal to the effective stress distribution at the time of sampling.

Unit III was sampled at two depths, and tests indicated that effective stress decreased with depth. A preconsolidation-stress range was assigned to layer 7 on the basis of this result. Layer 6 has a thickness of 18 m; hydraulic conductivity and storage properties are thought to be between those of the silty layers (1-5) and the clay layer (7). Layer 6 also is assigned a preconsolidation-stress range. All other layers are considered small enough and permeable enough so that a vertical

distribution of preconsolidation-stress values is not necessary. Because initial stress distributions were assumed, some error in computed values probably results from lack of knowledge about the distributions, particularly at the beginning of the simulation.

Calibration

Each layer at the extensometer site was simulated separately. The time-dependent compaction value for the fine-grained sediments and the instantaneous compaction value for the coarse-grained sediments were added to get the total daily compaction value. The data were then plotted as cumulative compaction versus time. The observed-compaction record from 1965 to 1983 was simulated. Observed data were plotted with simulated data to compare compaction values at the end of the period. The observed and simulated compaction rates also were compared. The values for hydraulic conductivity, specific storage, and preconsolidation stress were adjusted to calibrate the model to the observed field data.

Results

Model output and observed data were plotted as cumulative compaction versus time. Results were compared graphically (fig. 6) and statistically. The model output shown in figure 6 is the compaction simulation using the calibrated input parameters listed in table 1. A visual comparison of the observed and computed curves shows that the shapes match well throughout most of the period. The curves, however, diverge during long-term recovery and during the first 3 years of simulation. The total final compaction is within 0.015 m of the total compaction measured from 1965 to 1983. The mean difference between observed and computed compaction is 0.0038 m with a standard deviation of 0.0208 m.

The mean error is best understood when used in conjunction with the slope of the residual-error curve. The slope indicates how the difference between each observed and simulated value changes. A zero slope indicates a constant error. For this simulation the slope is small (-5.431×10^{-6} m/yr). The small negative slope indicates that simulated compaction will become increasingly less than observed compaction with time.

Aquifer-system compaction is simulated reasonably accurately over the entire period and during most annual cycles. In two situations, however, compaction is not accurately simulated. Large errors of about 50 mm are present during long-term recovery and during the first 3 years of the period. Compaction probably is overestimated for the first 3 years because 1965 is not the first year in which water levels decline. Because the preconsolidation stress is set equal to the water level of 1965, virgin compaction occurs throughout the first 150 days when water levels are falling. In reality, the preconsolidation stress probably is higher than the specified value and is exceeded later in the period. Increasing the preconsolidation stresses helped but did not remove the problem even when compaction became significantly underestimated throughout the rest of the period. The use of a preconsolidation-stress range in the two large layers (6 and 7) also reduced the initial compaction.

The second simulation error occurs during long-term water-level recovery. Unlike the annual recovery, overall recovery is not accurately simulated. Water levels rose significantly from 1972 to 1973 and from 1975 to 1979. During these two periods, water levels did not fluctuate enough to exceed previous preconsolidation stresses. The simulated aquitards expand and compact elastically, but the observed system appears to continue to compact virginally with only a slight decrease in compaction.

Three assumptions may contribute to the second simulation error. First, the assumption that the observed compaction is accurate to within the simulated errors may be incorrect. The extensometer may not be accurately measuring expansion-compaction during long-term recovery; therefore, the observed data may be incorrect. Measurement error might be studied by performing an aquifer test near the extensometer to define frictional problems in the equipment.

The second assumption is that the system is unconfined. Water-level data may have been measured in a confined zone. The water-level fluctuations measured in the 171 to 177-meter-depth interval are larger than might be expected for water-table fluctuations in the area. The water table probably fluctuates less, and part or all of the measured change is due to changes in artesian pressure. The effect of using the water-level fluctuations as water-table fluctuations is to overestimate stress changes occurring in the unconfined sections and to underestimate changes occurring in confined sections. Stress changes are overestimated in unconfined sections because the water table probably fluctuates less. Stress changes are underestimated in confined sections because a smaller percentage of the water-level change is used in calculating stress changes if the water level is considered a water table. In order to test the assumption that observed

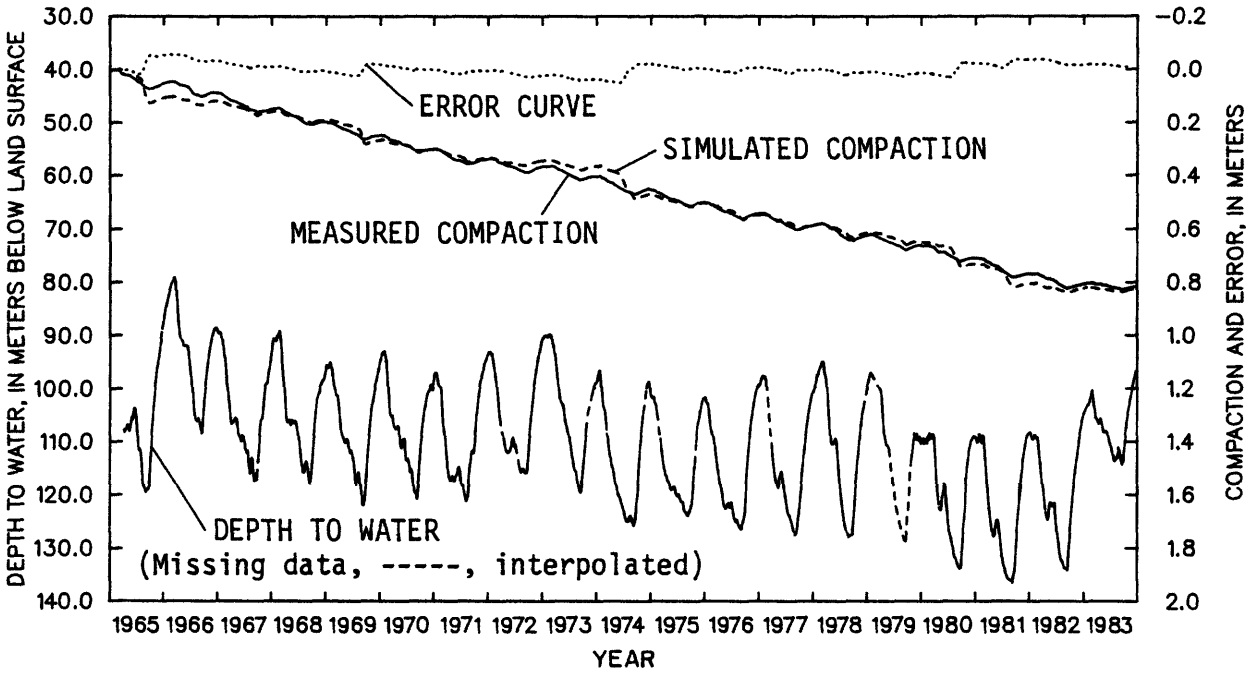

Figure 6.--Depth to water, simulated and measured compaction, and error curve at extensometer site.

water-level changes are equivalent to water-table changes, the system was modeled with different percentages of stress as contributed by water-level fluctuation for each depth. The percentage was lowest in the upper five layers and set equal to 100 for the lower two layers. The new stress distribution for the system had no effect on the problem of long-term recovery and increased the mean error to 0.0114 m and the standard deviation to 0.02164 m. The conclusion, therefore, was that the simulation was not improved by using water-level fluctuations instead of water-table fluctuations.

The third assumption is that an ongoing process can be accurately simulated after the process has started. This type of simulation does not account for the compaction caused by earlier changes in stress. The amount of ongoing compaction is related to the time constant for each layer. The virgin time constants for layers 1-5 do not exceed 1 year. The time constant for layer 6 is 3 years, which indicates that compaction caused by a stress change in 1962 may still be adding to compaction occurring in 1965. Assuming similar water-level fluctuations, this ongoing compaction would not exceed 0.03 m. Neglecting to include the amount of ongoing compaction would cause observed compaction to be underestimated by 3 percent. That error is nearly negligible; however, the error due to the large time constant of layer 7 (a maximum value of 35 years for the part of layer 7 in the well) may be more significant. The 35-year time constant indicates that compaction caused by stress increases after 1930 would continue well into the simulation period. Schumann and Poland (1970) estimated that compaction in the Eloy area began before 1962. It is difficult to determine when layer 7 began compacting. The residual compaction that could have occurred after 1965 would be even more difficult to calculate and could increase the percentage of the total compaction contributed by layer 7.

Examination of the total compaction contributed by each layer (fig. 7) in the model simulation indicated that layer 7 compacted linearly with respect to time and was almost insensitive to long-term recoveries similar to the overall trend of the system. Although layer 6 expanded in recovery periods in 1973 and 1979, layer 7 continued to compact. Simulated compaction in layer 6 initially dominated the system, but by 1972 compaction in layer 7 was as much or more than in layer 6. In summary, only layer 7 has a linear compaction rate similar to that observed for the system. If data had been available for simulation from about 1923, compaction in layer 7 would probably have dominated the system for the entire simulation period. The thickness of layer 6 and its virgin specific storage are greater than the thickness and virgin specific storage of layers 1 to 5; therefore, its compaction is large in relation to the compaction of layers 1 to 5. Layer 6 also has a high hydraulic conductivity in relation to layer 7; the high hydraulic conductivity causes compaction to occur rapidly. Layer 7 has a slower compaction rate and therefore may compact less than layer 6 in the short term. The ultimate total compaction in layer 7, however, is much greater than that in layer 6.

An actual compaction distribution among all 7 layers for 1965-83 probably is different from the simulated distribution. Layer 7 would have more compaction because of ongoing compaction from applied stress increases before 1965. The hydraulic-conductivity value for layer 6 may have been calibrated too high to account for ongoing compaction in layer 7. Ongoing compaction in layer 7 caused by applied stress increases prior to 1965 was

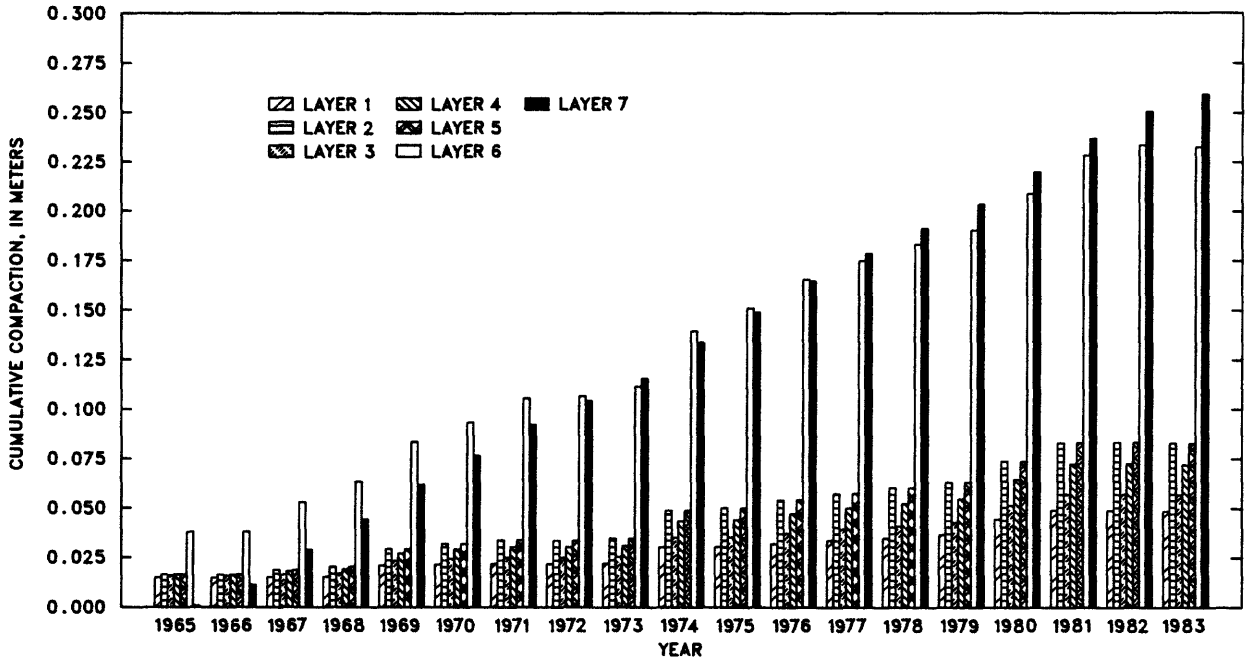

Figure 7.--Simulated annual cumulative compaction for each layer.

not included in the simulation. A laboratory test of the hydraulic conductivity of layer 6 is needed to confirm or correct the calibrated value.

The inaccurate distribution of compaction among all seven layers indicates a limitation of the Helm model. The model cannot account for ongoing compaction caused by stress changes prior to the start of the simulation period. As the time constant increases the distribution error caused by ongoing compaction increases. In order to accurately simulate compaction distribution using the Helm model, it is necessary to have water-level data extending back to initial water-level declines. The simulated system also should be composed of thin layers with time constants that are smaller than the simulation period.

Despite the uncertainties in initial conditions and problems simulating recovery, the overall simulation of compaction is reasonably accurate. For 1965-83, total simulated compaction is within 0.037 percent of the actual value. Layers 1 to 5 account for 39 percent of the total compaction measured at the extensometer for the simulation period. Layers 6 and 7 account for 29 and 32 percent of the total compaction, respectively.

Overall simulation of land subsidence was reasonably accurate (fig. 8) with a mean error of 0.011 m, which is less than 1 percent of the total measured land subsidence. Modeling land subsidence involved the simulation of compaction in layers 1 to 7. However the thickness of layer 7 was increased to 77 m, which includes sediments below the extensometer to a depth of 305 m. The hydraulic conductivity of layer 7 was set at 0.005 m/yr at the inner boundary to correct for a decrease in hydraulic conductivity with lithification. These changes increased the time constant to 355 years for layer 7. Only output for the dates on which leveling measurements were made are used for comparison in figure 8. The result of the simulation was that 50 percent of the total land subsidence occurred as compaction in layers 1 to 6 and 50 percent in layer 7.

Sensitivity Analysis

Four input parameters used to calibrate the model were varied by small amounts to measure the sensitivity of the model to the parameters. The parameters are preconsolidation stress, elastic and virgin specific storage, and hydraulic conductivity. Hydraulic conductivity and specific-storage values were separately increased and decreased by 20 percent for each layer, and the resultant mean-error and residual-slope values were calculated (table 2). The preconsolidation stress was altered by 5 percent. In order to understand the sensitivity of the model to changes in layers of different sizes, four types of simulations were performed for each property. The "small" simulation involves changing a given property in the smallest layer, 1, and observing its effect on the entire system without changing the other layers. The same method is followed for the "medium" layer, 6, and the "large" layer, 7. Finally, the property is altered in all layers to observe the combined effect.

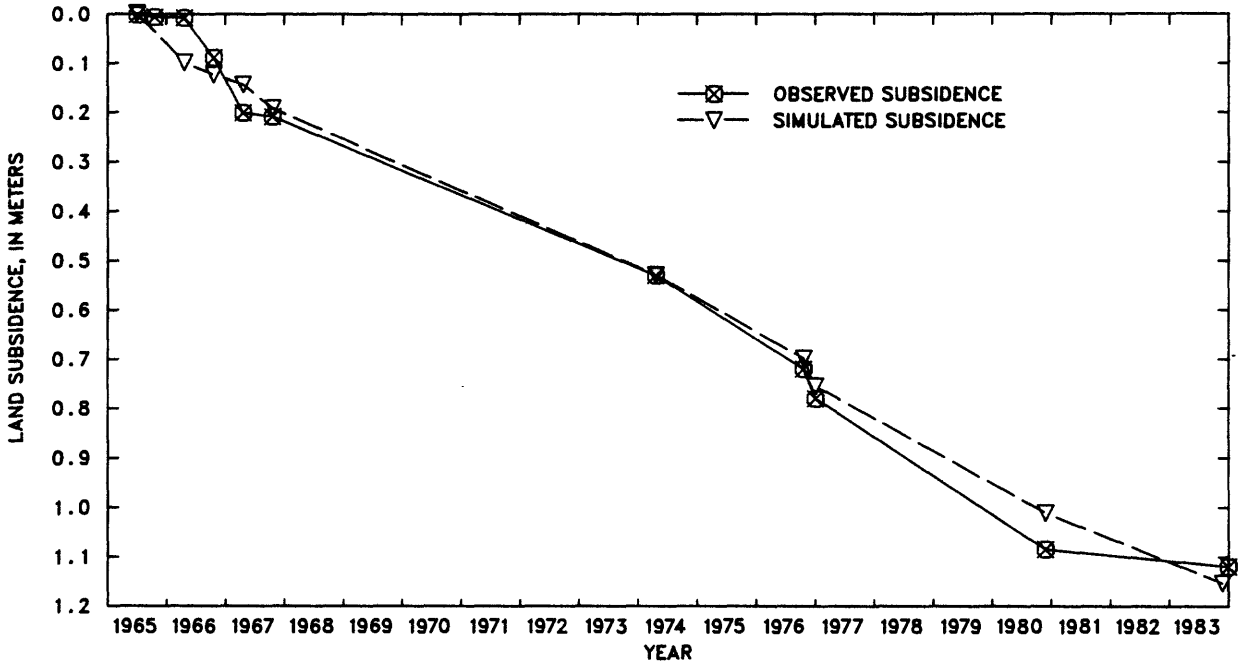

Figure 8.--Simulated and observed land subsidence at Eloy, Arizona.

On the basis of the percent change in mean error, the conclusion was that the model was most sensitive to preconsolidation stress and virgin specific storage. Half of the simulations have greater than 1,000-percent change when the stress is altered by only 5 percent. Decreasing the preconsolidation stress in layer 1 alone decreases the mean error by 589 percent. The mean error changes over 2,300 percent when virgin specific storage is increased or decreased in all layers by 20 percent.

The virgin specific storage of a layer can be related to its compressibility. Virgin specific storage represents the amount of water that can be released (per unit length) from a sediment. The model is sensitive to changes in the virgin specific storage, which affects the ultimate amount of compaction occurring in the system.

Model sensitivity to preconsolidation stress was confirmed because preconsolidation stress governs the time that virgin compaction begins. A 5-percent increase would change the initial preconsolidation stress by 5.50 m (depth to water in meters). The water level would have to drop 5.50 m below its initial point in order for virgin compaction to begin. With an overall water-level decline rate of 0.79 m/yr for 1965-83, virgin compaction would not begin until 6.96 years into the simulation period. Because elastic compaction would be occurring instead of virgin compaction, cumulative compaction would decrease significantly.

The mean error is improved in some simulations. In these simulations, hydraulic conductivity was decreased in layer 1 and in all layers combined and elastic specific storage was increased in layer 1. Although the mean-error value has improved in these simulations, the corresponding residual-slope values were worse. All slopes in these simulations increased (became more negative) indicating a greater divergence of simulated and observed data through time.

Changing some parameters did not consistently change the compaction simulation. Altering elastic specific storage and hydraulic conductivity sometimes had opposite effects on the total simulated compaction, depending on the type of layer in which the change was made. For example, decreasing the hydraulic conductivity in layer 7 decreased the total amount of simulated compaction from 1965-83. The average daily difference between observed cumulative compaction and simulated cumulative compaction increased 724 percent. The same change in layer 1 caused the average daily difference to decrease 185 percent indicating an increase in total compaction. The most significant differences between layer 7 and layer 1 are thickness, specific storage, and hydraulic conductivity. These three properties are used to calculate the time constant. A change in any of these properties changes the time constant accordingly. Decreasing the hydraulic conductivity increased the time constant of both layers. The time constant for layer 1, however, is small relative to the time constant for layer 7. The difference in time constants accounts for the same change in hydraulic conductivity which affects compaction in opposite ways. An increase in hydraulic conductivity for layer 7 increases the time constant and causes more compaction to be residual (compaction that continues after the simulation period ends), thereby decreasing the total compaction that occurs during the simulation period. In layer 1, the time constant does not increase beyond the length of the simulation period. Compaction is redistributed during the period but does not occur as residual compaction, therefore no compaction is deducted from the total compaction. The mean

Table 2.--*Results of sensitivity analysis*

Layer number	Mean error, in meters	Percent difference[1]	Standard deviation, in meters	Slope, in meters per year
		Hydraulic conductivity (-20 percent)		
1	-0.0039	-202.88	0.0208	-5.748×10^{-6}
6	-0.0059	-255.68	0.0209	-6.023×10^{-6}
7	-0.0191	-600.64	0.0228	-7.139×10^{-6}
All	-0.0249	-754.24	0.0233	-8.216×10^{-6}
		Hydraulic conductivity (-20 percent)		
1	-0.0033	-185.44	0.0207	-5.748×10^{-6}
6	0.0085	123.92	0.0207	-5.773×10^{-6}
7	0.0314	724.32	0.0203	-9.208×10^{-8}
All	-0.0020	-153.28	0.0220	-8.879×10^{-6}
		Virgin specific storage (+20 percent)		
1	-0.0109	-387.36	0.0022	-7.144×10^{-6}
6	-0.0277	-826.80	0.0263	-1.218×10^{-5}
7	-0.0113	-396.56	0.0224	-8.031×10^{-6}
All	0.0843	-2312.00	0.0427	-2.468×10^{-5}
		Virgin specific storage (-20 percent)		
1	0.0377	-0.96	0.0198	-4.465×10^{-6}
6	0.0302	693.84	0.0197	9.179×10^{-7}
7	0.0133	248.40	0.0197	-2.547×10^{-6}
All	0.0974	2456.16	0.0304	1.417×10^{-5}
		Elastic specific storage (+20 percent)		
1	-0.0034	-189.68	0.0208	-5.774×10^{-6}
6	0.0010	-73.28	0.0208	-5.630×10^{-6}
7	0.0062	63.60	0.2074	-5.520×10^{-6}
All	0.0125	228.96	0.0205	-5.221×10^{-6}
		Elastic specific storage (-20 percent)		
1	-0.0039	-201.68	0.0208	-5.827×10^{-6}
6	-0.0006	-115.44	0.0209	-5.777×10^{-6}
7	-0.0063	-266.16	0.0207	-5.524×10^{-6}
All	-0.0049	-228.88	0.0210	-5.608×10^{-6}
		Preconsolidation stress (+5 percent)		
1	0.0112	194.96	0.0208	-5.510×10^{-6}
6	0.0588	1442.40	0.0227	-4.124×10^{-6}
7	0.0169	343.28	0.0205	-3.813×10^{-6}
All	0.1870	4807.76	0.0307	-3.072×10^{-6}
		Preconsolidation stress (+5 percent)		
1	-0.0186	-588.96	0.0208	-6.023×10^{-6}
6	-0.0601	-1676.16	0.0214	-7.770×10^{-6}
7	-0.0170	-547.36	0.0214	-7.174×10^{-6}
All	-0.1829	-4899.52	0.0258	-1.019×10^{-5}

[1]Percent difference is difference between calibrated mean error and adjusted component mean error.

error improved with the redistribution of compaction, but the total compaction for the period did not increase. The change in layer 7 did decrease the total compaction by redistributing compaction beyond the simulation period. Ultimately, the amount of compaction is the same. For the simulation period, however, the amount of compaction decreases thus increasing the mean error

Increasing elastic specific storage in two layers with different properties also affects compaction in opposite ways. Increasing elastic specific storage in layer 1 decreases the mean error to the point where compaction is overestimated (indicated by a negative mean error). The same change in layer 7 increases the mean error slightly, and compaction is underestimated. The values of elastic specific storage are the same for both layers; however, the layer thickness and hydraulic conductivity combine to affect the way the specific storage is distributed. Altering layer 7 increased the total expansion occurring during periods of water-level recovery. Altering layer 1 increased the compaction occurring during periods when applied stresses were increasing below the preconsolidation stress.

On the basis of the sensitivity analysis, several conclusions can be made as to which factors affect compaction near Eloy. The virgin specific storage (or compressibility) and the preconsolidation stress are the two consistently sensitive parameters. Other parameters, such as hydraulic conductivity and elastic specific storage, can have varying effects on compaction depending on the type of layers that are involved. Changes in parameters in smaller layers with high hydraulic conductivities, such as layer 1, can affect the total amount and distribution of system compaction on a small scale; however, changes in layer 7 can affect compaction on a large scale. The thickness and compressibility of layer 7 and the fact that it is a singly draining layer result in a large time constant and make layer 7 an important component of this system.

The conclusions that virgin specific storage, preconsolidation stress, and layer 7 affect compaction can be extended to land subsidence. The compaction processes for layers 1-6 are the same in the land-subsidence simulation; however, layer 7 becomes an even more significant factor in controlling the system near Eloy because of its increased time constant.

SUMMARY

Compaction and land subsidence near Eloy, Arizona, from 1965 to 1983 were simulated with a one-dimensional model (Helm, 1972). The analysis included identification of seven compressible fine-grained layers. On the basis of this simulation, the upper 5 layers account for 39 percent of the total compaction measured at the extensometer for the 19-year period. The lower two layers account for 29 and 32 percent of the total compaction, respectively. Results of the simulation indicate that 50 percent of the total subsidence caused by compaction occurred in the upper six layers and 50 percent in the lowest layer.

A result of this study was the determination of which hydrologic and geologic factors most affect land subsidence near Eloy. From the sensitivity analysis, it was determined that the preconsolidation stress

and virgin specific storage were the two most significant properties for altering the compaction simulation. The large time constant for the lowest layer, which is mostly a function of thickness, makes this layer a factor in itself. The importance of this layer cannot be overestimated as it drives land subsidence. The time constant indicates that land subsidence may continue as a result of compaction in the lowest layer long after stresses stop increasing and other layers stop compacting.

Although the model reasonably simulates system compaction, more data are required to increase confidence in the resulting distribution of compaction among the layers. Daily water-level data before 1965 are needed to simulate ongoing compaction in the lowest layer, which has a time constant of 355 years for its entire thickness. Water-level data at several depths also are needed to better define the head distribution. Although the conclusion was made that the difference between water-level fluctuations and water-table fluctuations was not a significant factor in the simulation, head differences that are not constant with depth or time may contribute to forces such as seepage stresses that were neglected in this study. Laboratory tests of hydraulic conductivity conducted according to standard methods will determine if this parameter was set too high during calibration to account for compaction caused by other processes. Finally, the error involved in measuring compaction at the extensometer site can be determined by performing an aquifer test. The conclusion that virgin specific storage, preconsolidation stress, and the thick clay-rich layer 7 are important hydrologic and geologic factors may be useful in future studies of regional land subsidence and compaction in Picacho basin.

SELECTED REFERENCES

Davidson, E.S., 1971, Geohydrology and water resources of the Tucson basin, Arizona: U.S. Geological Survey Water-Supply Paper 1939-E, 81 p.

Eberly, L.D., and Stanley, T.B., 1978, Cenozoic stratigraphy and geologic history of southwestern Arizona: Geological Society of America Bulletin, v. 89, no. 6, p. 921-940.

Hardt, W.F., and Cattany, R.E., 1965, Description and analysis of the geohydrologic system in western Pinal County, Arizona: U.S. Geological Survey open-file report, 92 p.

Hardt, W.F., Cattany, R.E., and Kister, L.R., 1964, Basic ground-water data for western Pinal County, Arizona: Arizona State Land Department Water-Resources Report 18, 59 p.

Helm, D.C., 1972, Evaluation of stress-dependent aquitard parameters by simulating observed compaction from known stress history: Berkley, California, University of California, doctoral dissertation, 175 p.

_____1975, One-dimensional simulation of aquifer-system compaction near Pixley, California, 1. Constant parameters: American Geophysical Union, Water Resources Research, v. 11, no. 3, p. 465-478.

_____1976, One-dimensional simulation of aquifer-system compaction near Pixley, California, 2. Stress-dependent parameters: American Geophysical Union, Water Resources Research, vol. 12, no. 3, p. 375-391.

_____1977, Estimating parameters of compacting fine-grained interbeds within a confined aquifer system of one-dimensional simulation of field observations, in International Symposium on Land Subsidence, 2d, Anaheim, California 1976, Proceedings: International Association of Hydrological Sciences Publication 121, p.145-156.

_____1978, Field verification of a one-dimensional mathematical model for transient compaction and expansion of a confined aquifer system, in Specialty Conference on Verification of Mathematical and Physical Models in Hydraulic Engineering Proceedings: College Park, Maryland, American Society of Civil Engineers, p. 189-196.

Holzer, T.L., 1981, Preconsolidation stress of aquifer systems in areas of induced land subsidence: American Geophysical Union, Water Resources Research, v. 17, no. 3, p. 693-704.

Lofgren, B.E., 1969, Analysis of stresses causing land subsidence, in Geological Survey Research, 1968: U.S.Geological Survey Professional Paper 600-B, p. B219-B225.

Poland, J.F., Lofgren, B.E., and Riley, F.S., 1972, Glossary of selected terms useful in studies of the mechanics of aquifer systems and land subsidence due to fluid withdrawal: U.S. Geological Survey Water-Supply Paper 2025, 9 p.

Remson, I., Homberger, G.M., and Molz, F.J., 1971, Numerical methods in subsurface hydrology: New York, John Wiley and Sons, Inc., 389 p.

Riley, F.S., 1969, Analysis of borehole extensometer data from central California, in Tison, L.J., editor, Land Subsidence: Tokyo, International Association of Scientific Hydrology Publication 89, v. 2, p. 423-431.

Scarborough, R.B., and Peirce, H.W., 1978, Late Cenozoic basins of Arizona, in Callender, J.F., Wilt, J.C., and Clemons, R.E., editors, Land of Cochise: New Mexico Geological Society Guidebook, 29th Field Conference, p. 253-259

Schumann, H.H., 1986, Ground-water depletion and land subsidence in western Pinal County, Arizona: Focus Conference on Southwestern Ground Water Issues, October 20-22, 1986, Tempe, Arizona, Proceedings, p. 533-552.

Schumann, H.H., and Poland, J.F., 1970, Land subsidence, earth fissures, and ground-water withdrawal in south-central Arizona, U.S.A., in Land Subsidence: Tokoyo, International Association of Scientific Hydrology Publication 88, v. 1, p. 295-302.

Smith, G.E.P., 1938, The physiography of Arizona valleys and the occurrence of ground water: University of Arizona, College of Agriculture Technical Bulletin No. 77, 91 p.

Terzaghi, K., 1943, Theoretical soil mechanics: New York, John Wiley and Sons, Inc., 510 p.